Hindawi Publishing Corporation
International Journal of Chemical Engineering
Volume 2014, Article ID 474865, 7 pages
http://dx.doi.org/10.1155/2014/474865

Research Article

Analytical Simulation of Flow and Heat Transfer of Two-Phase Nanofluid (Stratified Flow Regime)

Mohammad Abbasi and Zahra Baniamerian

Department of Mechanical Engineering, Tafresh University of Technology, Tafresh 3951879611, Iran

Correspondence should be addressed to Zahra Baniamerian; amerian@tafreshu.ac.ir

Received 29 November 2013; Revised 9 February 2014; Accepted 10 February 2014; Published 25 March 2014

Academic Editor: Raghunath V. Chaudhari

Nanofluids have evoked immense interest from researchers all around the globe due to their numerous potential benefits and applications in important fields such as cooling electronic parts, cooling car engines and nuclear reactors. An analytical study of fluid flow of in-tube stratified regime of two-phase nanofluid has been carried out for CuO, Al_2O_2, TiO_3, and Au as applied nanoparticles in water as the base liquid. Liquid film thickness, convective heat transfer coefficient, and dryout length have been calculated. Among the considered nano particles, Al_2O_3 and TiO_2 because of providing more amounts of heat transfer along with longer lengths of dryout found as the most appropriate nanoparticles to achieve cooling objectives.

1. Introduction

Applying two-phase flows for providing more amount of heat transfer has been widely extended in last decades. Efficient cooling with two-phase flows requires a good knowledge of hydrodynamic and heat transfer behavior of flow regimes that in turn signify necessity of thermal and fluid modeling in this field. Use of nanoparticles combined with two-phase flows was found to considerably increase amounts of heat transfer and became a hot topic among researchers today. Some standard types of nanoparticles (TiO_2, CuO, Al_2O_3, and Au) are commonly employed, as well as what is applied in this study.

Excellent reviews are available on flow boiling; for example, Choi et al. [1] studied convective boiling using R-22, R-134a, and CO_2 in horizontal tubes. They stated that in low vapor qualities heat transfer coefficient is independent of mass flux. Increasing mass flux and also vapor quality from 40% to 70% enhanced heat transfer coefficient but in qualities from 70% to 100% heat transfer coefficient was decreased. Vapor quality is defined as the mass fraction of the vapor phase and is always between zero and one:

$$x = \frac{m_g}{m_l + m_g}. \quad (1)$$

Sur and Liu [2] observed significant differences between microchannels and conventional channels while examining two-phase flow properties. Gravity and viscous forces became less important compared to inertial forces and surface tension, so microchannels governing equations would be different from previous relations. Bubbly, annular, ring, and slug regimes were observed using channels with varied diameters. By decreasing diameter the difference between inertial forces and surface tension was increased.

Ozawa et al. [3] investigated flow pattern and boiling heat transfer of CO_2 in horizontal small-bore tubes. Regimes such as bubbly, annular, plug, wavy-annular, and slug-annular were observed. Dryout occurred at high heat flux and low mass flux and nucleate boiling was more important than convective boiling. Heat transfer coefficient was found related directly to heat flux and dependent on mass flux.

Baniamerian et al. [4] analytically modeled annular two-phase flow considering the four involved mass transfers. They employed empirical correlation to simulate heat transfer in annular flow regime and proposed correlations for pressure drop and mass transfer contributions individually.

Oueslati and Bennacer [5] investigated natural convection heat transfer of heterogeneous nanofluids. They found out that the highest values of heat transfer are obtained when

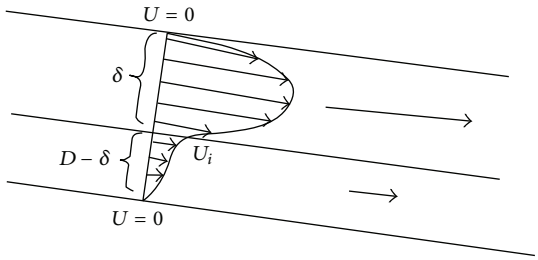

Figure 1: Lateral view of stratified flow.

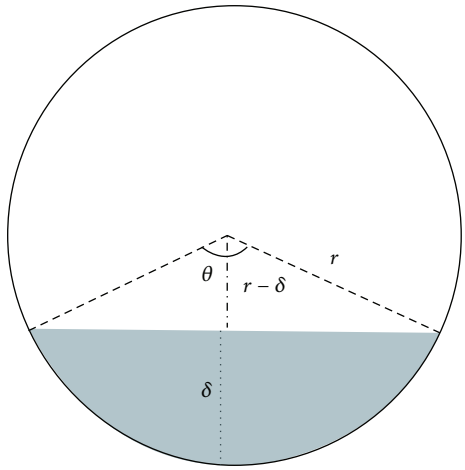

Figure 2: Pipe section.

using Cu nanoparticles. It was stated that the percentage of particle nature greatly affects the heat transfer and fluid flow.

Kim et al. [6] studied critical heat flux (CHF) enhancement in flow boiling using Al_2O_3 nanofluid. Maximum CHF enhancement was obtained at lowest mass flux and concluded that it is due to an increasing wettability of the heater surface and promoting liquid supply under bubbly or churn flow regime.

In another investigation, Witharana [7] studied the two-phase heat transfer performance of two types of Au and SiO_2-laden aqueous nanofluids in a cylindrical vessel under atmospheric pressure. It was stated that the boiling heat transfer increases and decreases for Au-nanofluid and SiO_2-nanofluid, respectively. These contradictory results are not well explained.

Xuan and Li [8] and Wen and Ding [9], by using Cu-water and Al_2O_3-water nanofluids, respectively, observed that heat transfer coefficient was enhanced by increasing volume fraction and Reynolds number.

In the present study two-phase flow with stratified flow regime of nanofluid is considered and simulated analytically. As mentioned before, the available models in two-phase field or nanofield are mostly experimental. In this regard an analytical model simulating stratified flow of nanofluid may be precious. Different nanofluids with similar two-phase flow regime (stratified) and similar geometrical conditions are simulated analytically. Nanofluids are compared from the viewpoints of heat transfer coefficient, dryout occurrence, and liquid film thickness variation.

2. Model Construction

Stratified flow regime of two-phase nanofluid in circular cross-section pipe is simulated analytically. A schematic of the stratified flow regime considered in this study is demonstrated in Figure 1. This regime is formed at low velocities of liquid and vapor and is used at cooling microdimension objects such as heat sinks. Some assumptions adopted in construction of the present two-dimensional analytical model are as follows.

(1) No-slip condition is assumed around the pipe wall.

(2) Velocity and position of liquid-vapor interface are unknown.

(3) Mass flow rate is constant.

(4) Pressure gradient of liquid and vapor phase is considered equal.

(5) Liquid region consists of water as the base liquid and nanoparticles which is assumed as a homogeneous fluid called nanofluid:

$$Q_L = u_L A_L, \qquad Q_G = u_G A_G. \tag{2}$$

Equations above point out the relation between volumetric mass flow, fluid velocity, and surface area of liquid and vapor phase.

Area of liquid element is calculated as follows:

$$A_L = \frac{r^2 (\theta - \sin(2\theta))}{2}. \tag{3}$$

As can be found from Figure 2 area of vapor element is

$$A_G = \frac{r^2}{2} (2\pi - (\theta - \sin 2\theta)), \tag{4}$$

where θ is the angle due to the liquid film thickness as demonstrated in Figure 2:

$$\theta = 2\cos^{-1}\left(\frac{r - h_l}{r}\right). \tag{5}$$

A control volume as shown in Figure 3 is considered in liquid region. The forces acting on this control volume consist of pressure force at both ends of the control volume, the momentum due to inlet and outlet mass flow rate, and shear stresses on the inner side of the pipe wall and on the interface between vapor and liquid. These forces are entirely shown in Figure 3.

Applying the exerted forces to derive momentum equation in liquid region results in the following relation:

$$0 = -h_L \left(\frac{dP}{dx} + \rho_L g \sin\theta\right) + \tau_{wL} + \tau_{iL}. \tag{6}$$

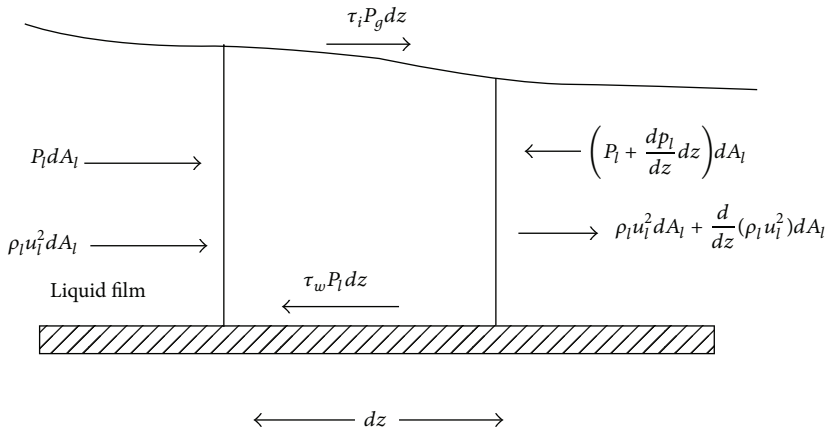

Figure 3: Momentum balance in liquid film.

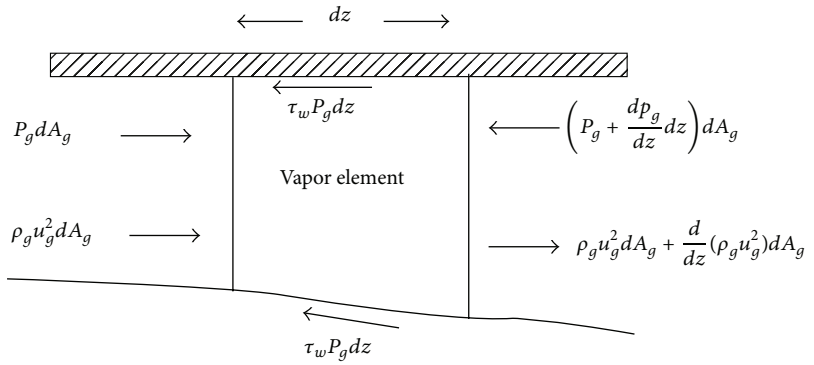

Figure 4: Momentum balance in vapor element.

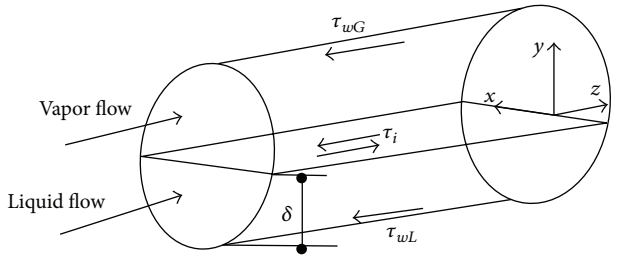

Figure 5: Shear stresses in pipe.

Performing what was previously mentioned for the vapor element based on the forces shown in Figure 4, the following correlation is obtained as the momentum balance:

$$0 = -h_G\left(\frac{dP}{dx} + \rho_G g \sin\theta\right) + \tau_{wG} + \tau_{iG}. \tag{7}$$

Shear stresses are demonstrated in Figure 5. As the interfacial stresses experienced by liquid and vapor elements are equal:

$$\sum_{k=L,G} \tau_{ik} = 0. \tag{8}$$

Pressure gradient of liquid and vapor phase is considered equal based on assumption (4). Considering (6)–(8) along with assumption (4), the following relation will result:

$$\left(\rho_L - \rho_G\right) g \sin\theta = \frac{\tau_{wL} - \tau_{iG}}{h_L} - \frac{\tau_{wG} + \tau_{iG}}{h_G}. \tag{9}$$

Wall shear forces due to both liquid flow and vapor flow can be calculated by employing the following [10]:

$$\tau_{wL} = -\frac{\mu_L}{h_L}\left(6U_L - 2U_i\right), \tag{10}$$

$$\tau_{wG} = -\frac{\mu_G}{h_G}\left(6U_G - 2U_i\right). \tag{11}$$

Another correlation is available to calculate shear force on the interface [10]. The correlation is applied once for the interfacial stress due to liquid region and then due to vapor region although they are equal in act:

$$\begin{aligned} \tau_{iL} &= \frac{\mu_L}{h_L}\left(6U_L - 4U_i\right), \\ \tau_{iG} &= -\frac{\mu_G}{h_G}\left(6U_G - 4U_i\right). \end{aligned} \tag{12}$$

Gas viscosity is much lower than liquid viscosity. It can be concluded from (12) that

$$\mu_G \ll \mu_L \longrightarrow U_i = \frac{3}{2}\mu_L. \tag{13}$$

Substituting the above magnitude for the interfacial velocity in (12),

$$\begin{aligned} \tau_{iG} = & -\tau_{iL} = -6\frac{U_G - U_L}{(h_G/\mu_G) + (h_L/\mu_L)} \longrightarrow \tau_{iG} \\ \approx & -6\frac{\mu_G}{h_G}(U_G - U_L), \\ T_{wL} \approx & -6\frac{\mu_L}{h_L}U_L - \tau_{iG}. \end{aligned} \tag{14}$$

3. Heat Transfer Computations

Many researches have been carried out in order to model heat transfer in two-phase flows. Among the numerical and experimental investigations, many presented empirical correlations are used to compute heat transfer coefficient in two-phase heat transfer. In present study Kandlikar's correlation is used to compute heat transfer coefficient [11, 12]. This correlation is the most suitable one to the present study since it has been obtained based on several experiments accomplished for various kinds of refrigerants. Those are very similar to nanofluids employed in this study from the view point of thermophysical properties. The correlation is of the following form:

$$\begin{aligned} h &= \text{Maximum of } h_{\text{nb}}, h_{\text{cb}}, \\ h_{\text{nb}} &= 0.6683\text{Co}^{-0.2}h_l + 1058\text{Bo}^{0.7}F_{fl}h_l, \\ h_{\text{cb}} &= 1.136\text{Co}^{-0.9} + 667.2\text{Bo}^{0.7}F_{fl}h_l, \\ \text{Co} &= \left\{\left[\frac{1}{x} - 1\right]^{0.8}\left(\frac{\rho_g}{\rho_l}\right)^{0.5}\right\}, \\ \text{Bo} &= \frac{q''_{ch}}{G \cdot h_{fg}}, \\ F_{fl} &= 1 \quad \text{For water}, \\ h_l &= 0.023\text{Re}_l^{0.8}\text{Pr}_l^{0.4}\left(\frac{k_l}{D}\right), \\ \text{Re}_l &= \frac{G(1-x)D}{\mu_l}, \\ \text{Pr}_l &= \frac{\mu_l C_{pl}}{k_l}, \\ x &= \frac{m_g}{m_l + m_g} = \frac{\rho_g V_g}{\rho_l V_l + \rho_g V_g}. \end{aligned} \tag{15}$$

4. Modeling Nanofluid

In order to simulate nanofluid flow, the flow is assumed to be uniform. Therefor, nanofluid is supposed as a homogenous mixture and all of its thermophysical properties are calculated through an average of nanoparticles properties and the base fluid properties. The average is dependent largely on particles volume fraction. There are several methods for calculating the thermophysical properties of nanofluids which are obtained by several averaging methods.

One of the most important parameters that can be changed by adding nanoparticles to the base fluid is the fluid conductivity. This is due to primary objective of creating nanofluids which is enhancing fluid conductivity by adding metallic nanoparticles. One of the well-known correlations for computing conductivity heat transfer coefficient is given [13]:

$$k_{\text{nf}} = k_f\left[\frac{k_p + (n-1)k_f - (n-1)\phi\left(k_f - k_p\right)}{k_p + (n-1)k_f + \phi\left(k_f - k_p\right)}\right]. \tag{16}$$

"n" accounts for shape factor that is considered equal to 3 for spherical nanoparticles,

$$\mu_{\text{nf}} = \mu_f\left(1 + 2.5\phi + 6.2\phi^2\right). \tag{17}$$

According to the above relation, dynamic viscosity of nanofluid is just dependent on volume fraction of nanoparticle and fluid viscosity. Nanofluid heat capacity at constant pressure and density is calculated as follows:

$$\begin{aligned} C_{p-\text{nf}} &= \phi C_{p-p} + (1-\phi)C_{p-f}, \\ \rho_{p-\text{nf}} &= \phi\rho_p + (1-\phi)\rho_f. \end{aligned} \tag{18}$$

5. Solution Procedure

Two-phase stratified regime is modeled through conducting a program written in Matlab programming environment. In this program two values for the liquid film thickness are guessed and then by knowing pipe geometry two amounts for vapor thickness are obtained. By having liquid and vapor velocity as input, (11) can be used to obtain vapor-liquid interface velocity. Then the wall and interfacial shear stresses can be achieved by employing (10)–(12). Finally, relationship (8) can be used to verify the initial guess accuracy. Eventually by using Newton's bisection method, liquid film thickness is computed. If the thickness of initial guesses were incorrect, the guesses should be altered and above steps are repeated. Thermophysical data applied in this study are tabulated and shown in Table 1.

6. Model Verification

The present model is verified with the pioneering work of Ursenbacher et al. [15]. Ursenbacher et al. developed a model based on nonintrusive computerized image analysis and optical observation method to detect the vapor-liquid interface in stratified two-phase pure flows. They introduced

Table 1: Thermophysical properties of refrigerants and particles [14].

Refrigerant/metal	Temperature (K)	Pressure (MPa)	Density (Kg/m^3)	C_p (KJ/Kg·K)	K (W/m·K)	Viscosity (Pa·s)	Evaporation enthalpy (KJ/Kg)	Surface tension (N/m)
Water (L)	300	3.169	996.5	4.181	0.6103	8.53×10^{-4}	2438	0.0717
Vapor	300	3.169	0.02559			0.99×10^{-5}		
Cu	293		8933	385	401			
Al_2O_3	293		3970	765	40			
Gold	293		19320	129	318			
TiO_2	293		4250	686.2	8.9538			

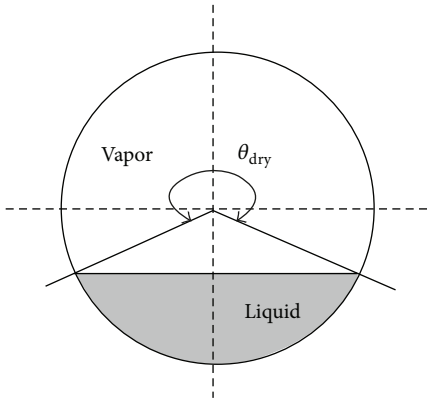

Figure 6: Schematic of dry angle for stratified flow regime in pipe.

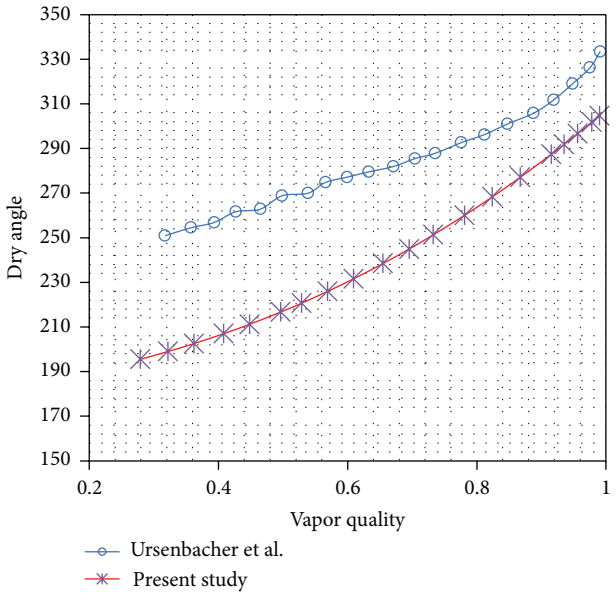

Figure 7: Comparison between results of the present study and results derived by Ursenbacher et al. [15].

a parameter named "dry angle" (θ_{dry}) that is shown in Figure 6.By turning the effects of nanoparticles off in the present model, results are compared to those of Ursenbacher et al. for the same working fluid and flow conditions (the applied working fluid is R22 in a pipe of 1.58 cm diameter).

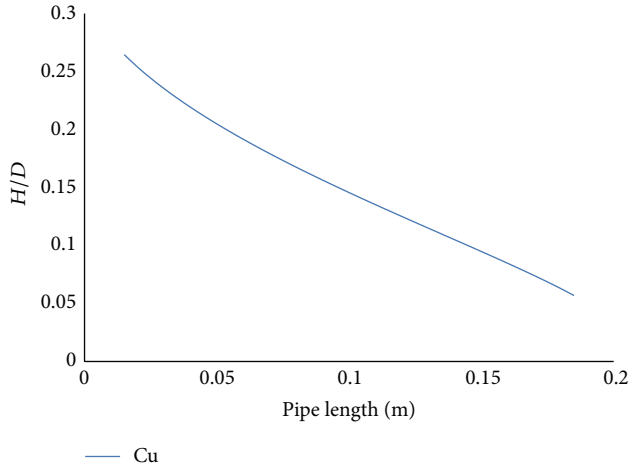

Figure 8: Variation of liquid film thickness against the pipe length for nanofluid with copper nanoparticles.

Variations of dry angle against vapor quality for various mass flow velocities are obtained and compared to what is presented by Ursenbacher et al. and good agreement has been concluded. A comparison for typical mass velocity of 100 kg/m^{2}s is accomplished and demonstrated in Figure 7. Average deviation of 16.4% is found between the models.

7. Results and Discussion

Nanoparticles of copper, gold, titanium oxide, and aluminum oxide are applied in this study to produce nanofluid with water as the base fluid. Each nanofluid is supposed to flow in 1-meter pipe of 0.0512 m diameter with liquid film and vapor velocities of 0.00084 m/s and 0.01686 m/s to assure experiencing a stable stratified flow regime as reported by de Sampaio et al. [16]. The pipe is exposed to uniform wall heat flux of 10 kJ/m^2 from its sidelong.

The objective is to have a comparison between heat transfer coefficient and dryout length of different nanofluids considered in this study. For this reason volume fraction of nanoparticles in all investigated nanofluids is considered 1%.

Figure 8 shows variation of liquid film thickness against pipe length. As determined the thickness is reduced along the pipe due to evaporation until it reaches the limit defined as the critical thickness in the model. The defined limit is 0.003

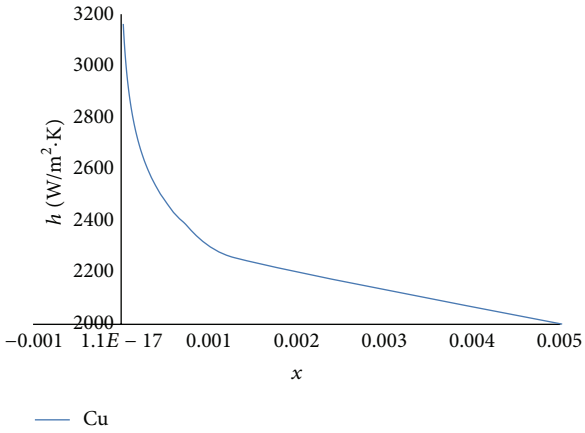

Figure 9: Variation of heat transfer coefficient against quality for nanofluid with copper nanoparticle.

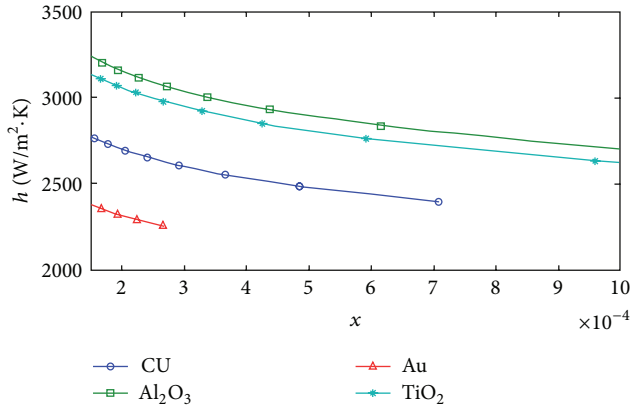

Figure 11: Variation of heat transfer coefficient against quality for all nanoparticles.

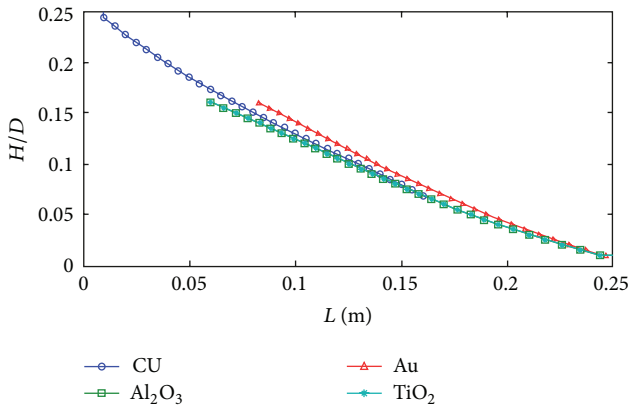

Figure 10: Variation of liquid film thickness against the pipe length for all nanoparticles.

of pipe section. Decreasing the liquid film thickness up to the specified level expresses the dryout occurrence and the length of pipe corresponding to the critical thickness is known as dryout length. The dryout length is obtained: 0.21 of the pipe total length.

Heat transfer coefficient is computed by Kandlikar's correlation [11, 12]. Variation of heat transfer coefficient against copper-nanofluid quality is demonstrated in Figure 8.

In two-phase flows heat transfer coefficient often decreases along the flow as the vapor quality increases. This issue has been investigated in this study for the two-phase (boiling) nanofluid, and it is found as shown in Figure 9 that applying nanofluid instead of a pure fluid does not influence this behavior of two-phase systems.

A brief comparison is accomplished for different employed nanofluids with similar operating and thermal conditions. Heat transfer coefficient and dryout length for each nanofluid are plotted and demonstrated together in Figures 10 and 11.

8. Conclusion

Variation of liquid film thickness and heat transfer coefficient for copper oxide, gold, aluminum oxide, and titanium oxide are shown, respectively, in Figures 10 and 11.

Al_2O_3 and TiO_2, because of providing more amount of heat transfer coefficient along with longer length of dryout, are proffered over other considered nanofluids. In most of researches Au and Cu are commonly the providers of maximum heat transfer among nanoparticles while in the present study because of considering stratified regime and due to low velocity condition Al_2O_3 and TiO_2 surpass the two mentioned nanoparticles because of their lower densities which reduces possibilities of sedimentation.

Regarding what was previously mentioned, it can be declared that the most suitable nanoparticle for construction of the nanofluid directly depends on the flow regime as well as fluid properties.

Nomenclature

A: Area
Bo: Boiling number
Co: Convection number
C_p: Specific heat at constant pressure
D: Tube diameter
F_{fl}: Fluid-dependent parameter
G: Mass flux
h: Convective heat transfer coefficient
H: Liquid film thickness
h_{fg}: Latent enthalpy of evaporation
k: Thermal conductivity
L: Tube length
m: Mass
P: Pressure
Pr: Prandtl number
q: Heat flux
Q: Volumetric flow rate
r: Radius

Re: Reynolds number
u: Velocity
We: Weber number
x: Quality.

Greek Symbols

δ: Liquid film thickness
θ: Angle
ρ: Density
τ: Shear stress
μ: Dynamic viscosity
σ: Surface tension
Φ: Volume fraction.

Subscripts

cb: Convective boiling
f: Fluid
g: Vapor
i: Inner
l: Liquid
nb: Nucleate boiling
nf: Nanofluid
w: Wall.

Conflict of Interests

The authors declare that there is no conflict of interests regarding the publication of this paper.

References

[1] K.-I. Choi, A. S. Pamitran, C.-Y. Oh, and J.-T. Oh, "Boiling heat transfer of R-22, R-134a, and CO_2 in horizontal smooth minichannels," *International Journal of Refrigeration*, vol. 30, no. 8, pp. 1336–1346, 2007.

[2] A. Sur and D. Liu, "Adiabatic air-water two-phase flow in circular microchannels," *International Journal of Thermal Sciences*, vol. 53, pp. 18–34, 2012.

[3] M. Ozawa, T. Ami, I. Ishihara et al., "Flow pattern and boiling heat transfer of CO_2 in horizontal small-bore tubes," *International Journal of Multiphase Flow*, vol. 35, no. 8, pp. 699–709, 2009.

[4] Z. Baniamerian, R. Mehdipour, and C. Aghanajafi, "Analytical simulation of annular two-phase flow considering the four involved mass transfers," *Journal of Fluids Engineering*, vol. 134, no. 8, Article ID 081301.

[5] F. S. Oueslati and R. Bennacer, "Heterogeneous nanofluids: natural convection heat transfer enhancement," *Nanoscale Research Letters*, vol. 6, no. 1, p. -11, 2011.

[6] T. I. Kim, Y. H. Jeong, and S. H. Chang, "An experimental study on CHF enhancement in flow boiling using Al_2O_3 nano-fluid," *International Journal of Heat and Mass Transfer*, vol. 53, no. 5-6, pp. 1015–1022, 2010.

[7] S. Witharana, *Boiling of refrigerants on enhanced surfaces and boiling of nanofluids [Ph.D. thesis]*, Royal Institute of Technology, 2003.

[8] Y. Xuan and Q. Li, "Investigation on convective heat transfer and flow features of nanofluids," *Journal of Heat Transfer*, vol. 125, no. 1, pp. 151–155, 2003.

[9] D. Wen and Y. Ding, "Experimental investigation into convective heat transfer of nanofluids at the entrance region under laminar flow conditions," *International Journal of Heat and Mass Transfer*, vol. 47, no. 24, pp. 5181–5188, 2004.

[10] *Modelling and Control of Two-Phase Flow Phenomena*, International Centre for Mechanical Science, Udine, Italy, 2002.

[11] S. G. Kandlikar, "General correlation for saturated two-phase flow boiling heat transfer inside horizontal and vertical tubes," *Journal of Heat Transfer*, vol. 112, no. 1, pp. 219–228, 1990.

[12] S. G. Kandlikar, "Model for flow boiling heat transfer in augmented tubes and compact evaporators," in *Proceedings of the Winter Annual Meeting*, November 1990.

[13] S. M. S. Murshed, C. A. Nieto De Castro, M. J. V. Loureno, M. L. M. Lopes, and F. J. V. Santos, "A review of boiling and convective heat transfer with nanofluids," *Renewable and Sustainable Energy Reviews*, vol. 15, no. 5, pp. 2342–2354, 2011.

[14] ASHRAE Handbook, American Society of Heating, Refrigerating and Air-conditioning Engineers, 2005.

[15] T. Ursenbacher, L. Wojtan, and J. R. Thome, "Interfacial measurements in stratified types of flow. Part I: new optical measurement technique and dry angle measurements," *International Journal of Multiphase Flow*, vol. 30, no. 2, pp. 107–124, 2004.

[16] P. A. B. de Sampaio, J. L. H. Faccini, and J. Su, "Modelling of stratified gas-liquid two-phase flow in horizontal circular pipes," *International Journal of Heat and Mass Transfer*, vol. 51, no. 11-12, pp. 2752–2761, 2008.